Numerical and experimental investigation of the optical connectivity technique in cross flow atomization

G. Charalampous, C. Hadjiyiannis, Y. Hardalupas*
Mechanical Engineering Department, Imperial College London, UK
georgios.charalampous@imperial.ac.uk, c.hadjiyiannis09@imperial.ac.uk and
y.hardalupas@imperial.ac.uk

Abstract

The optical connectivity technique has been proposed for the characterization of the morphology of continuous liquid jets before breakup. The technique is based on internal illumination of a liquid jet by a laser beam through the spray nozzle. The liquid jet acts as a light guide and the laser beam propagates along the length of the jet in the same way that light travels along the length of an optical fibre. The laser beam excites a fluorescent dye that is dissolved in the liquid jet, making the volume of the liquid jet luminous. However, unlike an optical fibre, there are laser beam intensity losses along the length of the liquid stream due to refraction at the liquid/gas interface and due to absorption by the fluorescence dye. While the technique has been shown to work well in 'straight' jets, for liquid jets exposed to a cross stream of air, where the liquid jet becomes gradually inclined relative to the axis of the jet exit, laser light losses due to refraction through the liquid interface may increase and lead to limitations of the technique. An investigation of the performance of the optical connectivity is conducted for liquid jets exposed to a cross stream of air. First, numerical simulations of the light propagation within inclined liquid columns for various geometries of the liquid jet are presented. The numerical investigation is supplemented by an experimental application of optical connectivity to a liquid jet exposed to a cross-stream of air.

Introduction

During the initial stages of atomization of a liquid jet, the jet is destabilized under the influence of the forces from the interaction of the liquid stream with the surrounding air [1]. The morphology of an initially 'straight' liquid jet changes as is perturbed by a coaxial gas flow and liquid is removed from its surface [2-3]. This process continues until the liquid stream becomes completely discontinuous. The extent of this region defines the "primary atomization region". The evolution of the jet morphology in this region is important, since it determines the final droplet size distribution of the spray. For this region a number of optical diagnostic techniques have been developed to probe this process.

Some of the techniques for the characterization of the continuous jet include photography [2-3], electrical conductivity [4-6], X-ray absorption [7-8] and ballistic imaging [9-10]. A novel technique in this category is the optical connectivity technique [11-12]. It has the advantage that it can probe in dense sprays and provide a good visualization of a continuous liquid jet at conditions where the atomization products surrounding the continuous liquid jet could limit the optical access for photographic or shadowgraphic studies.

However, there are limitations to the applicability of the optical connectivity technique. The inevitable losses of the laser beam intensity due to refraction at the gas-liquid interface will reduce the amount of light that illuminates the liquid jet downstream of the nozzle. Therefore, the remaining laser light intensity in the liquid jet may be insufficient to provide adequate excitation of the fluorescent dye till the breakup region. For 'inclined' liquid jets, the losses due to refraction may become more significant than for 'straight' jets as more of the laser light rays meet the liquid interface at large angles.

It is the purpose of this paper to examine the applicability of the optical connectivity technique to 'inclined' jets. First, we extend the numerical model of [13] which evaluates the propagation of a laser beam and the resulting fluorescent intensity along the length of a straight liquid column for inclined column. In this way, we can determine how the laser light that is introduced at the base of a jet propagates along the length of the 'inclined' jet and what are the effects of its geometry on the fluorescent intensity profile along the jet length. Then, we investigate the continuity of the liquid stream exposed to a cross stream of air and evaluate the implications on the applicability of the optical connectivity technique to this type of flows.

The optical connectivity technique

The optical connectivity technique is based on the introduction of a laser beam upstream of the spray nozzle [11]. The laser light that exits through the nozzle in the direction of the liquid flow is guided by the liquid jet

* Corresponding author: y.hardalupas@imperial.ac.uk

downstream, by reflection on the liquid interface. When the angle of incidence is greater then the angle of total internal reflection:

$$\theta_{crit} = \sin^{-1}\left(\frac{n_2}{n_1}\right) \quad \textbf{(1)}$$

where n_1, n_2 the refractive indices of the liquid and the gas phases, the beam is completely reflected back inside the liquid at an angle that is equal to the angle of incidence. This is similar to the propagation of light within an optical fibre. However, if the angle of incidence becomes smaller than that for total internal reflection, some of the laser light escapes through refraction at an angle determined by Snell's law:

$$\frac{\sin\theta_1}{\sin\theta_2} = \frac{n_2}{n_1} \quad \textbf{(2)}$$

where θ_1 is the angle of incidence on the surface and θ_2 is the angle of refraction (Figure 1). In this case the intensity of the laser beam within the liquid jet decreases.

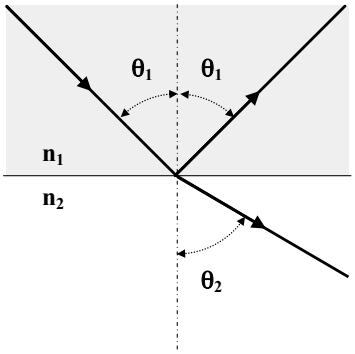

Figure 1: Reflection and refraction of a ray incident on the interface at an angle θ_1.

At the breaking point of the liquid jet, the propagation of the laser beam along the jet length is interrupted and the light cannot be contained within the jet and diffuses widely. By adding a fluorescing dye into the liquid, some of the laser beam intensity is absorbed as the laser beam travels along the length of the liquid jet. The absorbed light is then re-emitted as fluorescence. The process is shown schematically in Figure 2. Since fluorescence is spectrally shifted to wavelengths that are longer than the excitation wavelength, with the addition of an optical filter in front of the camera lens the scattered light can be suppressed and the luminous core of the spray can be imaged without background noise from the scattered light.

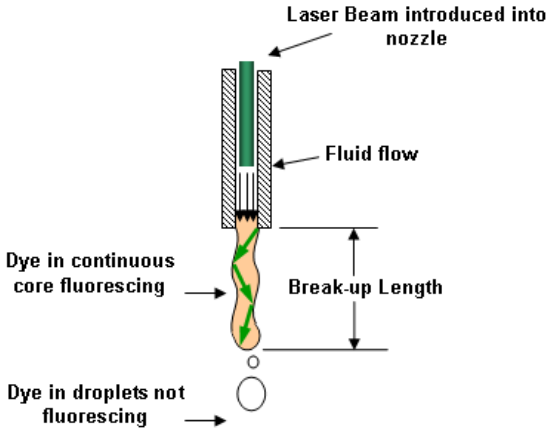

Figure 2 Principle of the optical connectivity technique.

The intensity losses of the laser beam along the continuous length of the jet depend on the liquid jet structure. If a jet has a smooth surface there are few scattering losses and the emitted fluorescent intensity from the jet is fairly uniform along the continuous length of the jet. If, on the other hand, the jet surface is rough, the scattering losses are significant and the laser light intensity diminishes with distance from the nozzle. As a result, the fluorescent intensity decreases with distance from the nozzle [13]. Therefore, depending on the geometry of the jet, there are limits on the length of the continuous jet that can be visualized with the optical connectivity technique.

The additional distortion of the jet when it is placed in a cross stream of gas is expected to cause increased losses of the laser beam intensity along the jet length and potentially limit the applicability of the technique.

Numerical approach

A numerical simulation of the laser beam propagation within the liquid jet can evaluate the effect of influencing parameters independently on the performance of the optical connectivity technique. Such experimental investigation is difficult to realise. The liquid column interface is described by a sinusoidal function along the X-axis of a Cartesian coordinate system:

$$Y = G \cdot \sin\left(\frac{2\pi X}{\lambda}\right) + a \cdot \left(\frac{X}{50}\right)^2 + y_0 \quad \textbf{(3)}$$

where G is the amplitude of the wave on the interface and λ is the wavelength of the wave on the surface of the column. The offset in the equation is the distance that the liquid interface is displaced from the central axis coordinate system at the base of the column. By considering an offset of 0.5 and -0.5 for the top and bottom boundaries respectively, the base of the liquid column is unity. The inclination of the jet relative to the X-axis is controlled by parameter α. When α is zero, the liquid is a 'straight' column. For α≠0, a quadratic deflection is introduced on the column centreline, which increases with increasing α.

The laser beam that propagates inside the liquid column is simulated using a large number of rays that start at the base of the jet and propagate downstream the nozzle exit. The rays are not always parallel to the X-axis but can diverge to account for the divergence of the laser beam. The rays interacting with the interface are reflected back at an angle that is equal to the angle of incidence (Figure 1). An example of the path of the rays inside 'straight' and 'inclined' columns with similar geometrical characteristics is presented in Figure 3, which demonstrates the influence of the inclination.

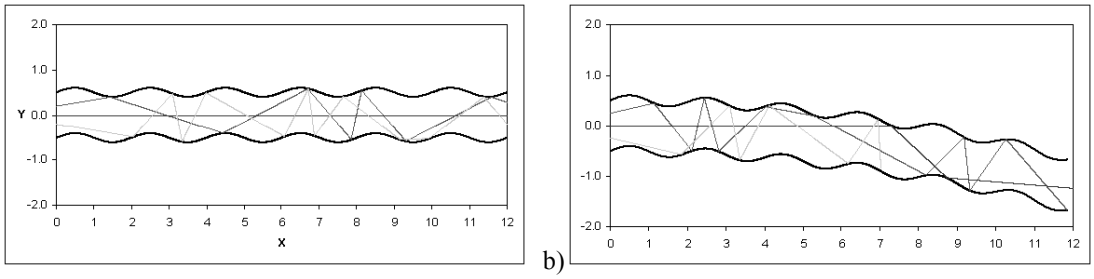

Figure 3: Example of propagation of light rays within a) 'straight' and b) 'inclined' liquid column, as determined by ray tracing.

As the rays propagate inside the liquid column, the initial intensity of each beam I_0 is reduced due to absorption of light by the fluorescent dye in the liquid and refraction of light at the liquid interface when the angle of incidence of the rays on the surface of the column is smaller than the critical angle for total internal reflection. The reduction of the intensity of the rays due to the absorption caused by the medium through which the ray is travelling is estimated by the Beer-Lambert law:

$$I = I_0 e^{-\gamma z} \quad \textbf{(4)}$$

where γ is the absorption coefficient, z the distance travelled by the ray, I_0 is the initial intensity of the ray and I the intensity of the ray after it has travelled a distance z in the absorbing medium.

The Fresnel equations are used to calculate the fraction of the incident ray intensity R that is reflected back into the liquid. The Fresnel coefficients depend on the polarisation of the incident ray. If the electric field of light is perpendicular to the plane of incidence, the reflection coefficient is:

$$R_s = \left[\frac{\sin\left(\theta_1 - \theta_2\right)}{\sin\left(\theta_1 + \theta_2\right)}\right]^2 \quad \textbf{(5)}$$

If the electric field of light is parallel to the plane of incidence, the reflection coefficient R is:

$$R_p = \left[\frac{\tan\left(\theta_1 - \theta_2\right)}{\tan\left(\theta_1 + \theta_2\right)}\right]^2 \quad \textbf{(6)}$$

and the overall reflectance R is equal to the mean of R_s and R_p.

$$R = \frac{R_p + R_s}{2} \quad (7)$$

The conditions under which the numerical simulations were performed are summarised in the table below. The absorption cross section of the liquid was deliberately chosen to be small, in order to avoid considerable decrease of the fluorescent intensity close to the base of the column due to absorption.

Table 1: Numerical simulation parameters	
n1	1.33
n2	1.0
L	0.5, 1.0, 2.0
G	0.1
a	00, 10, 20, 30
Divergence	0°, 10°
γ	0.0001

Experimental arrangement

For the experimental investigation, a cross-flow air-blast atomizer was used that was specifically designed to accommodate optical connectivity. A schematic of the cross section of the atomiser is presented in Figure 4.

The air flow was supplied by four inlets at the far end of a cylindrical plenum chamber (9). The chamber was closed at the far end by a plate (7) and, at the other side, it was connected to a contraction (3) of 38mm exit diameter that accelerated the air flow. The contraction ended in a straight nozzle (1), which was extended by a straight quartz tube (8). The quartz tube contained the air flow stream and, in addition, allowed optical access to the flow. It is within the length of the quartz tube that the atomization of the liquid jet takes place and can be studied, while the surrounding air flow velocity remains constant. The assembly of the above components comprised the main body of the atomiser.

The atomizing liquid was delivered by a long straight steel tube of circular cross-section (2) with 8mm external diameter. The tube was supported along the centreline of the atomiser main body. One end (6) of the tube was connected to the liquid supply, while the other end was closed. A circular hole was drilled at the side of the tube normal to the tube centreline at the start of the transparent nozzle (Figure 4, detail). In this way, a liquid jet could be injected normal to the air flow within the bounds of the transparent nozzle. The annular gap between the central tube and the quartz tube was 15mm. For the implementation of the optical connectivity technique, an optical window (14) was placed on the liquid delivery tube immediately opposite to the liquid exit, as shown in the detail at bottom right of Figure 4. In combination with the transparent straight nozzle of the air flow, direct optical access was obtained at the back of the liquid injection orifice, so that a laser beam can be directed into the liquid jet and the optical connectivity technique applied.

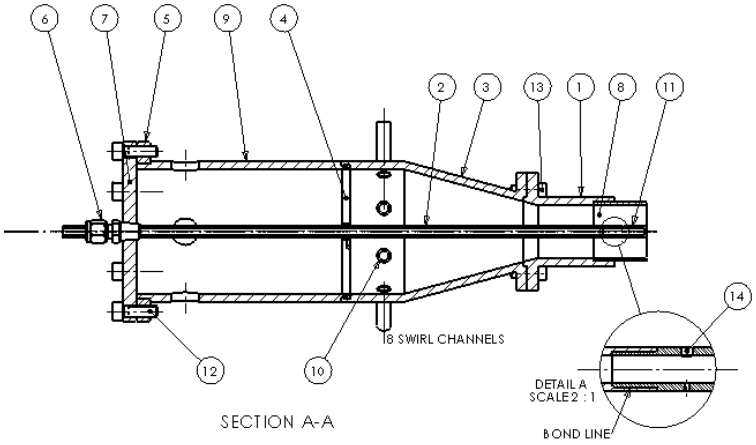

Figure 4: Schematic of atomizer of liquid jet exposed to a cross stream of air. Detail at bottom right shows design of liquid nozzle exit and optical window.

The atomized liquid in this investigation was water, doped with Rhodamine WT fluorescing dye. The fluorescent dye was excited by the second harmonic of a Nd:YAG laser beam at 532nm. The laser beam was focused on the optical window behind the liquid nozzle exit, so that some of the laser light was transmitted through the

nozzle and into the liquid jet. The fluorescent intensity images emitted by the liquid jet were recorded by a 12-bit PCO sensicam QE CCD camera. The camera lens was fitted with an OG590 optical filter, which suppresses the scattered light at 532nm but allows transmission of the red-shifted fluorescence spectrum of the dye.

The considered flow conditions are summarized in Table 2 below. The chosen air and liquid velocities were a compromise between introducing sufficient deflection on the liquid jet to avoid impingement of the jet on the quartz tube wall and simultaneously preventing filming along the length of the liquid delivery tube. In total 10 flow conditions were considered and for all flow conditions 500 image samples were acquired.

Table 2: Flow conditions

U_{Liquid}	U_{Gas}	Re	We	U_{Liquid}	U_{Gas}	Re	We
m/s	m/s			m/s	m/s		
2.1	21.5	1895	7.7	3.2	27.7	2842	12.8
2.1	24.6	1895	10.1	3.2	30.8	2842	15.8
2.1	27.7	1895	12.8	3.2	33.8	2842	19.1
2.1	30.8	1895	15.8	3.2	36.9	2842	22.7
2.1	33.8	1895	19.1	3.2	40.0	2842	26.7

Results and discussion

From the numerical calculations of the ray propagation and absorption within the liquid column, the fluorescent intensity along the length of the column was calculated by integrating the amount of absorbed light intensity across the transverse (Y-axis) cross-section of the column. The fluorescent intensity was considered to be directly proportional to the absorbed light. The fluorescent intensity profiles are presented using the moving average of the fluorescent intensity over a range of one jet base diameter along the X-axis to remove oscillations of the fluorescent light intensity and highlight the overall trends.

From the fluorescent intensity profiles presented in Figure 5, a number of significant differences in the evolution of fluorescent intensity can be observed that depend on the column geometry and the divergence of the laser beam. The most profound effects on the distribution of fluorescent intensity along the column length are a consequence of the divergence of the laser beam. When the beam is collimated (Figure 5, left column), the fluorescent intensity along the liquid column is initially exhibiting an exponential decrease. After some distance from the column base, the decrease of the fluorescent intensity follows a parabolic function. This pattern persists until the fluorescent intensity of the column becomes minimal. From this point on, the fluorescent intensity decrease follows an exponential function. Also, there is significant differentiation of the fluorescent intensity profiles with respect to the amount of deflection from the centreline, as greater amounts of deflection cause the fluorescent intensity emitted from the liquid column to decrease more rapidly with distance from the column base.

In contrast to the case of the collimated beam, when the light rays are diverging, the fluorescent intensity along the length of the liquid column decreases according to an exponential fashion (Figure 5, right column) for the entire length of the column. In addition, in the presence of laser beam divergence, the differences between the fluorescent intensity profiles of jets become largely independent of the amount of inclination of the column.

The development of the fluorescent intensity profile can be interpreted in terms of the propagation of the light rays in the column. In the case of a collimated beam in a straight column, only a few of the rays impinge on the interfacial waves close to the base of the column. Some of them impinge at angles that are smaller than the angle for total internal reflection and immediately scatter outside the column, resulting in some immediate losses of laser light while the rest propagate further along the liquid column and scatter gradually. This is the mechanism that is responsible for the initial exponential decay of fluorescent intensity. The wavelength of the surface instability plays a significant role here. Shorter waves cause the exponential decay to develop within a short distance from the column base as the rougher interface makes it more likely that the rays will impinge of the column surface at an angle that is smaller than the angle of total internal reflection and scatter. Longer wavelengths of surface instabilities make it more likely that the non-diverging rays will interact with the smoother surface at an angle that is greater than the angle for total internal reflection and continue to propagate along a greater distance of the initial length of the column. In the case of the non-deflected column, past the initial fluorescent intensity decrease there are no more significant losses since the absorption due to the fluorescent dye is small and the rays do not further interact with the interface. In this case, the fluorescent intensity along the remaining column length is uniform. This is also the case for instability wavelength L=2.0, although the initial decrease of the fluorescent intensity is not complete within the examined length and cannot be seen in Figure 5. When the column is deflected, there is a transition from the initially exponential fluorescent intensity decay to parabolic intensity decay. The decrease becomes more profound as the deflection of the column increases. This is because a significant number of parallel rays, which impinge on the liquid interface at angles of incidence smaller than the angle for total internal reflection and, therefore, there is a rapid loss of intensity due to refraction.

The observations change considerably when the rays at the base of the column are diverging. Because of the divergence of the rays, many of them interact with the liquid interface at angles that are less than the angle for total internal reflection. This causes rapid fluorescent intensity losses close to the base of the column, which persist along the rest of its length. Even for straight columns, there is a continuous decrease of the fluorescent intensity along the column length. However, the variance in the direction of the ray causes the fluorescent intensity along the column length to become largely insensitive to the instability wavelength and the deflection of the column. In fact, for this reason, the fluorescent intensity at the end of the column is greater for the more deflected columns when the rays are divergent than collimated.

Continuing to the experimental results, for the purposes of this investigation, which is the evaluation of the performance of the optical connectivity technique on deflected jets, we focus on the development of the mean fluorescent intensity across the liquid jet length as it can be compared with the numerical results. Despite the difference between the infinite length jet that was considered in the numerical investigation and the finite length jet of the experimental investigation which is limited by both the height of the annular gap in which the jet develops, which is 15 jet diameters here, and the breakup of the jet due to atomisation the general conclusions of the former investigation can be applied to the latter.

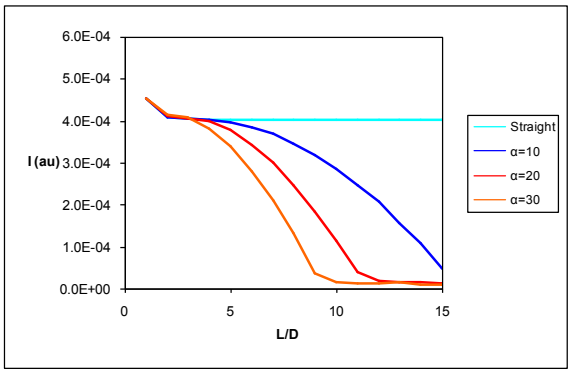

G=0.1, L=0.5, γ=0.0001, no laser beam divergence

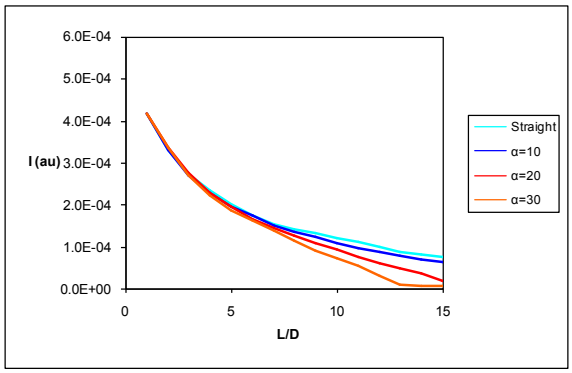

G=0.1, L=0.5, γ=0.0001, 10° laser beam divergence

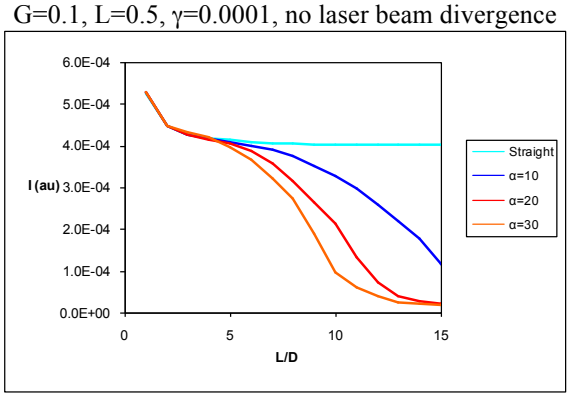

G=0.1, L=1.0, γ=0.0001, no laser beam divergence

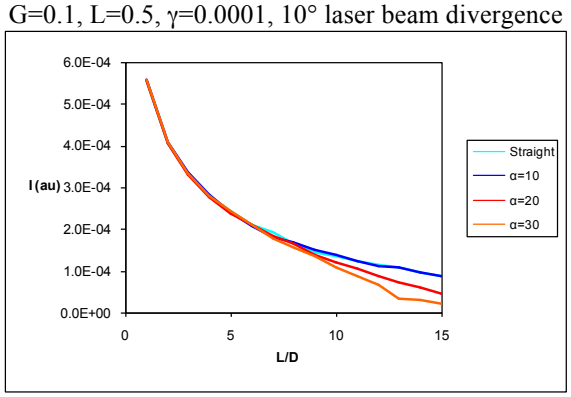

G=0.1, L=1.0, γ=0.0001, 10° laser beam divergence

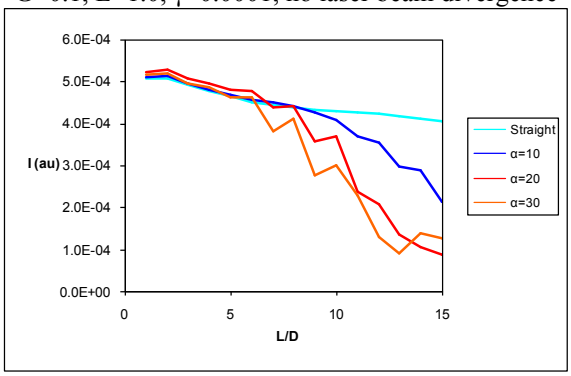

G=0.1, L=2.0, γ=0.0001, no laser beam divergence

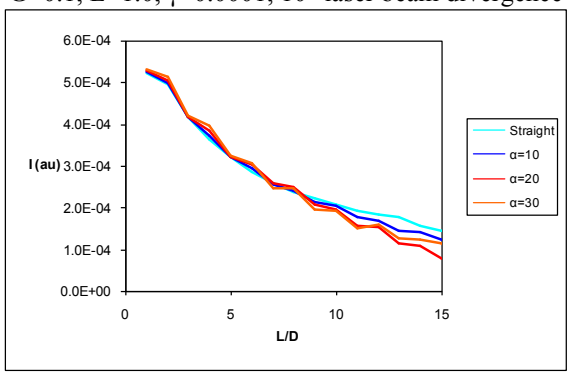

G=0.1, L=2.0, γ=0.0001, 10° laser beam divergence

Figure 5: Numerically calculated profiles of fluorescent intensity along the length of straight and inclined liquid columns.

The images of the mean fluorescent intensities along the jet core in Figure 6 andFigure **7** show that the deflected jets can be visualised for a considerable length even in cases where the deflection of the jet reaches al-

most 90°. However the inclination of the jet imposes some limitations on the propagation of the illuminating laser light through the jet volume. The most apparent effect of inclination is that the fluorescent intensity of the jet is not uniform throughout the jet volume. Close to the point of maximum inflection of the jet, the fluorescent intensity is always increased along an oblique line through the jet. This is significant since the images shown in the figures represent the mean intensity of 500 samples. Therefore, this intensity distribution is not a coincidental occurrence but a temporally persistent characteristic of the jet visualisation that prevails over the particular details of the individual image samples. It can be explained by considering that the illuminating beam is deflected on the curved interface at certain angles that depend on the inclination of the jet. In this case, much of the reflected light is concentrated along a narrow strip of the jet increasing the local fluorescent intensity.

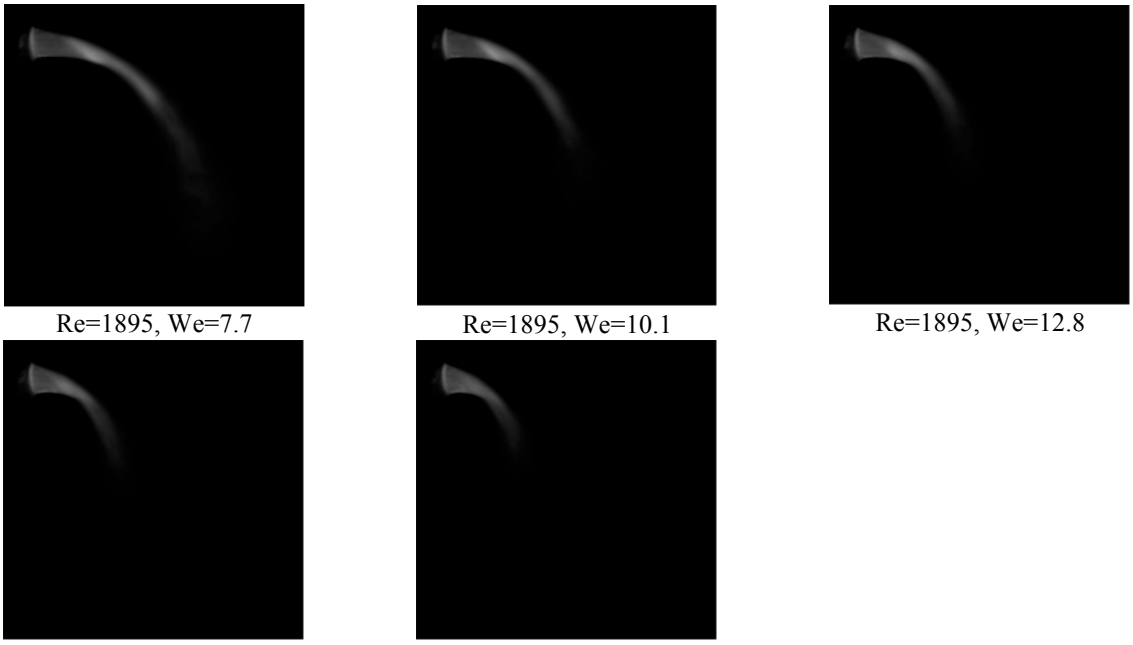

Figure 6: Experimentally measured mean fluorescent intensity emitted by the liquid jet for Re=1895.

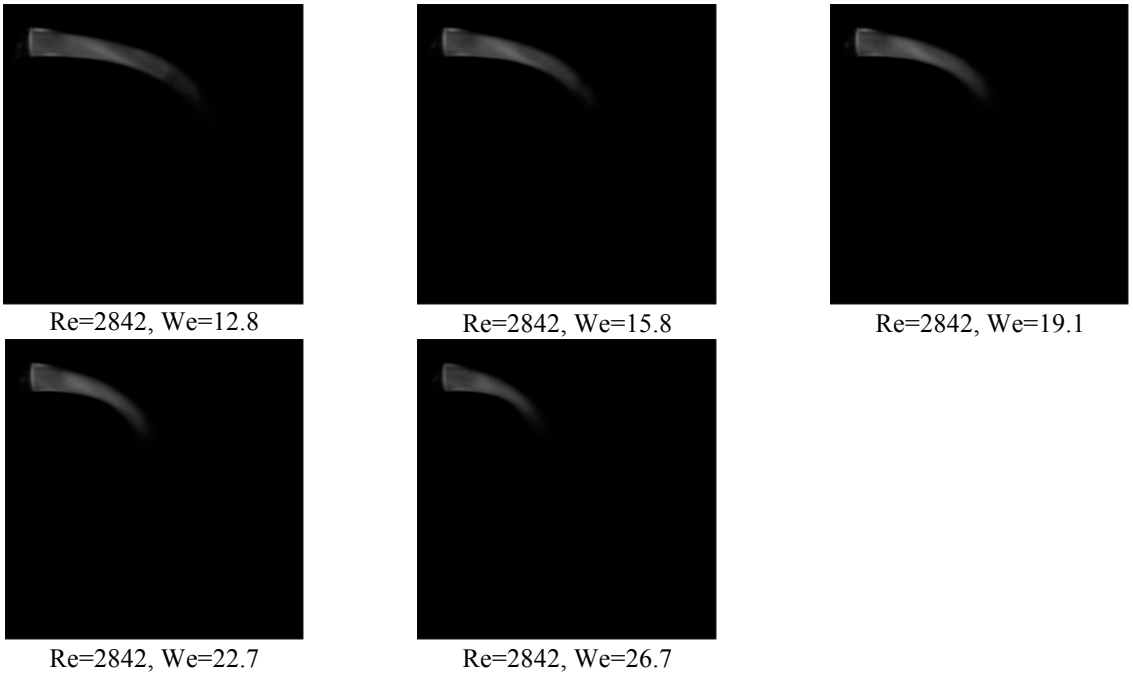

Figure 7: Experimentally measured mean fluorescent intensity emitted by the liquid jet for Re=2842.

From the mean intensity images of the jet, the mean fluorescent intensity profiles are calculated by evaluating the mean fluorescent intensity along the jet cross-section and presented in Figure 8. Comparison with the

profiles of Figure 5 shows that there are some differences, which can be attributed to the more complex geometry of real jets. Nevertheless, they can be explained in the same way as discussed in the numerical simulation results.

The initial development of the fluorescent intensity profile shows an increase of the fluorescent intensity, which peaks at the point of maximum jet inflection. After this point an exponential decrease of the fluorescent intensity follows for the remaining length of the jet. While the fluorescent intensity profiles do not overlap with each other, it can be observed that with the exemption of Re=1896, We=7.7 in all other cases the rate of decrease of the fluorescent intensity is almost identical. This suggests that the laser light losses of the illuminating laser beam become independent of the details of the jet geometry. As before, this can be explained by a considerable number of rays from the illuminating beam interacting with the interface at angles that are less than the angle for total internal reflection, which is in agreement with the numerical simulations as it is unlikely that the illuminating beam in our experimental implementation is collimated at the base of the jet.

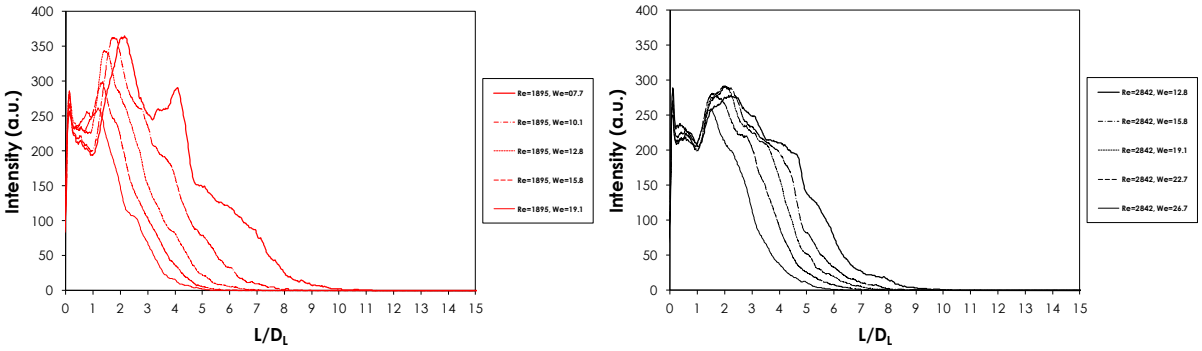

Figure 8: Cross-section averaged fluorescent intensity profiles along the length of the liquid jet for liquid jet Reynolds numbers Re=1895 (left) and Re=2842 (right)

Conclusions

Numerical and experimental investigations were conducted to evaluate the performance of the optical connectivity technique applied to jets that are deflected from a straight path, as is the case of jet development exposed to cross-flow air stream. The numerical investigation revealed that the fluorescent intensity profiles along the liquid column length are highly sensitive to the divergence of the illuminating laser beam. In addition, the wavelength of the surface instability and deflection of the jet had a significant effect on the fluorescent intensity profiles only for a collimated illuminating laser beam. The experimental investigation showed that the fluorescent intensity is not uniformly distributed throughout the volume of the jet but a fluorescent intensity maximum exists at the point of maximum jet inflection. The rate of decay of the fluorescent intensity along the length of the jet is similar among the jets regardless of the length of the jet, which suggests that after the jet maximum inflection, there are considerable losses of the illuminating laser beam intensity due to refraction.

References

[1] Lefebvre, A. H. *Atomization and sprays*: Hemisphere Publishing Corporation, 1989.
[2] Engelbert, C., Hardalupas, Y., and Whitelaw, J. H., *Proceedings of the Royal Society of London Series A-Mathematical and Physical Sciences* 451: 189-229, (1995).
[3] Varga, C. M., Lasheras, J. C., and Hopfinger, E. J., *Journal of Fluid Mechanics* 497: 405-434, (2003).
[4] Hiroyasu, H., Shimizu, M., and Arai, M., *ICLASS-82*, (1982).
[5] Chehroudi, B., Chen, S. H., and Bracco, F. V., *SAE Technical Papers 850126*, (1985).
[6] Yule, A. J., and Salters, D. G., *Atomization and Sprays* 4: 41-63, (1994).
[7] Cai, W. Y., Powell, C. F., Yue, Y., Narayanan, S., Wang, J., Tate, M. W., Renzi, M. J., Ercan, A., Fontes, E., and Gruner, S. M., *Applied Physics Letters* 83: 1671-1673, (2003).
[8] Renzi, M. J., Tate, M. W., Ercan, A., Gruner, S. M., Fontes, E., Powell, C. F., MacPhee, A. G., Narayanan, S., Wang, J., Yue, Y., and Cuenca, R., *Review of Scientific Instruments* 73: 1621-1624, (2002).
[9] Linne, M. A., Paciaroni, M., Gord, J. R., and Meyer, T. R., *Applied Optics* 44: 6627-6634, (2005).
[10] Paciaroni, M., Linne, M., Hall, T., Delplanque, J. P., and Parker, T., *Atomization and Sprays* 16: 51-69, (2006).
[11] Charalampous, G., Hardalupas, Y., and Taylor, A. M. K. P., *AIAA Journal* 47: 2605-2615, (2009).
[12] Charalampous, G., Hardalupas, Y., and Taylor, A., *International Journal of Spray and Combustion Dynamics* 1: 389-415, (2009).
[13] Charalampous, G., Hardalupas, Y., and Taylor, A. M. K. P., *48th AIAA Aerospace Sciences Meeting*, Orlando, Florida, Jan. 4-7, 2010